2-1-2020

Characterizing Intersection Variability of Butterfly Diagram in Post-stroke Gait Using Kernel Density Estimation

Yun Ju Lee
Tsing Hua University

Jing Nong Liang
University of Nevada, Las Vegas, jingnong.liang@unlv.edu

Gait & Posture 76 (2020) 157–161

Contents lists available at ScienceDirect

Gait & Posture

journal homepage: www.elsevier.com/locate/gaitpost

Characterizing intersection variability of butterfly diagram in post-stroke gait using Kernel Density Estimation

Yun-Ju Lee[a], Jing Nong Liang[b,*]

[a] Department of Industrial Engineering and Engineering, Management National Tsing Hua University No. 101, Section 2, Guangfu Road, East District, Hsinchu City, 300 Taiwan

[b] Department of Physical Therapy, University of Nevada, Las Vegas 4505 S Maryland Pkwy, Box 453029 Las Vegas, NV 89154 USA

ARTICLE INFO

Keywords:
Butterfly diagram
Center of pressure
Gait
Kernel Density Estimation
Locomotor variability

ABSTRACT

Background: Center of pressure (COP) trajectory during treadmill walking have been commonly presented using the butterfly diagram to describe gait characteristics in neurologically intact and impaired individuals. However, due to the large amount of displayed information, the butterfly diagram is not an efficient solution to visualize locomotor variability.

Purpose: The purpose of this study was to evaluate post-stroke locomotor variability by applying Kernel density estimation (KDE) on the intersections of the butterfly diagram, and to compare KDE derived metrics with conventional metrics of gait symmetry and variability.

Methods: Bilateral toe-off (TO) and initial contact (IC) points of the butterfly diagram were determined to calculate the COP symmetry index and the intersections of bilateral TO−IC. Subsequently, the intersections during the walking window were used to evaluate its density and variability by Kernel density estimation. Standard deviations of step width and step length were compared between groups.

Results: Using the KDE surface plots we observed 4 characteristically different patterns with individuals post-stroke, which were associated with functional status quantified using walking speed and lower extremity Fugl-Meyer scores. However, locomotor variability quantified using standard deviations of step width and lengths did not differ between groups.

Significance & Novelty: This paper presents a novel approach of using KDE analysis as a better and more sensitive method to characterize locomotor COP variability in individuals with post-stroke hemiparesis, compared to conventional metrics of gait symmetry and variability.

1. Introduction

Gait variability and symmetry are commonly used as quantifiable measures of mobility, in the non-neurologically impaired elderly or neurologically-impaired individuals [1–4]. Distinctive gait variabilities have been reported for different neurological conditions [2,5–7]. Earlier studies examining post-stroke locomotor control have reported significant asymmetry and variability in all aspects of neuromuscular control during locomotion, including step length asymmetry, step width asymmetry, activation and coordination of lower extremity muscles and foot-force regulation, [2,3,6,8,9]. These are associated with activity and mobility restrictions, and increased risk for falls [4,10,11]. Reliable techniques to characterize variability in gait parameters are clinically important for assessing fall risks, or used as performance measures for evaluating responses to interventions, as well as for the design and follow-up of rehabilitative programs [12].

Center of pressure (COP) trajectory during walking is commonly represented using the butterfly diagram. Previous research used the butterfly diagram to present essential gait characteristics, such as variability, stride width, and symmetry between legs [13,14]. Furthermore, the butterfly diagram showed high repeatability of spatio-temporal parameters during treadmill walking and running [15]. In the lab, walking on an instrumented treadmill could overcome disadvantages of overground walking, such as long distance or walking period. It creates a characteristic feature as an intersection of the butterfly diagram, which is defined as the point determined by two diagonal COP displacement from initial contact (IC) to the consecutive contralateral toe off (TO), and is indicative of the temporal and spatial components of gait variability with the locations of bilateral feet positions. The standard deviations of the intersection points in the anterior/

* Corresponding author.
E-mail addresses: yunjulee@ie.nthu.edu.tw (Y.-J. Lee), jingnong.liang@unlv.edu (J.N. Liang).

https://doi.org/10.1016/j.gaitpost.2019.12.005
Received 26 June 2019; Received in revised form 23 October 2019; Accepted 5 December 2019

posterior and lateral directions have been associated with gait variability [14]. However, this approach was disregarding the relationship between the intersection and feet positions, and potentially underestimates the effects of asymmetric gait pattern, particularly in individuals with post-stroke hemiparesis.

Using binary regression analysis on the butterfly diagram, it is possible to distinguish lower anterior-posterior (AP) and medial-lateral (ML) variability in individuals with very mild Expanded Disability Status Score (EDSS) from the rest of the EDSS levels [14]. However, there still remain limitations in distinguishing locomotor variability within the neurologically-impaired population, for instance, gait deficits due to weakness in multiple sclerosis [4,16] have different characteristics compared to that in individuals with post-stroke hemiparesis.

Kernel Density Estimation (KDE) is a well-established statistical approach often used to estimate the probability density of datasets in geometric features, econometrics and pattern recognition [17–19]. KDE applied in point pattern analysis, was used to evaluate spatial distributions of diseases in epidemiology [20,21] and traffic accidents in a network space [22]. A smooth density surface was used to represent point events over studying area and the occurrence rate. Additionally, KDE was used with a diffusion process and outperformed its accuracy and reliability in two-dimensional cases [23]. Similarly, KDE can be used to determine the spatial probability distribution of the intersections in the butterfly diagram. To date, the KDE approach has not been applied to evaluate gait performances to distinguish variability between individuals with and without neurologic impairments. Since the KDE approach is used to calculate the occurrence and distribution of events of interest within the target area, when applied to butterfly diagrams, the intersections are comparable with the events of interest, and the four points of bilateral IC and TO referred to the target area. Therefore, the KDE approach could potentially reveal gait variability and provide quantitative values for better understanding of neurologically-impaired gait patterns.

This study aimed to evaluate walking variability in individuals with chronic post-stroke hemiparesis by applying KDE on the intersections of the conventional butterfly diagram. Our primary objective was to use KDE analysis to explore characterization of the spatial probability distribution of intersections in the butterfly diagram during walking in individuals with post-stroke hemiparesis and non-neurologically impaired controls. Additionally, we sought to compare the metrics derived from KDE analysis with conventional metrics of gait symmetry and variability.

2. Methods

2.1. Participants

Ten individuals (4 females, 6 males; 72.4 ± 7.9(mean ± SD)years old), who have sustained a single, unilateral cortical or subcortical stroke, more than 6 months (8.3 ± 9.0years) before the study, and had residual lower limb hemiparesis on the left side, participated in this study. Ten age-similar non-neurologically impaired individuals (6 females, 4 males; 59.36 ± 11.45 years old) were recruited as controls.

Individuals post-stroke were recruited only if they were able to walk on the treadmill independently without assistive devices. Participants were excluded if they had other neurological conditions, orthopedic conditions affecting walking, or history of hip or knee replacement. Each participant received written and verbal information about the experiment procedures before giving written consent. The protocol was approved by the Institutional Review Board at the University of Nevada, Las Vegas.

2.2. Experimental protocol

Participants wore a safety harness attached to an overhead support, and walked on a dual belt instrumented treadmill (Bertec Corp, Columbus OH). The safety harness was attached to the overhead support with some slack, serving as a safety mechanism in case of a fall and did not support any body weight during walking. Body weight was recorded during static standing on the dual belt treadmill. We first determined each individual's self-selected walking speed on the instrumented treadmill. Once the self-selected walking speed was determined, each individual walked for 60 s. Ground reaction forces were sampled at 2000 Hz.

2.3. Data processing

All ground reaction forces (GRF), moments and COP data were processed and analyzed offline using custom MATLAB programs (Mathworks, Natick, MA). GRFs were filtered with a 30 Hz low-pass, 4th order, zero-lag Butterworth filter. X_{left} and Y_{left} represented the COP trajectory on the left belt; X_{right} and Y_{right} represented the COP trajectory on the right belt. Subsequently, COP_x and COP_y were calculated from the force plates of the left and right belts by weighting average:

$$COP_x = \frac{x_{left}F_{z-left} + x_{right}F_{z-right}}{F_{z-left} + F_{z-right}}$$

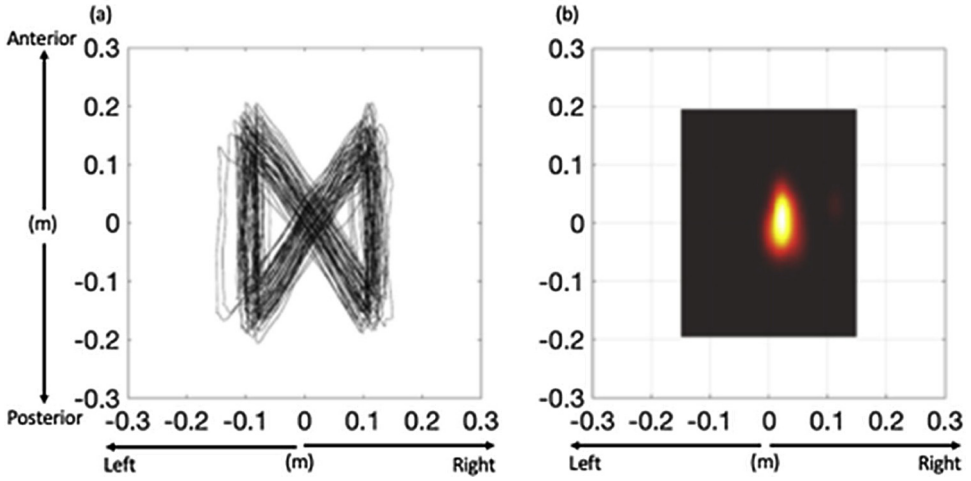

Fig. 1. The COP trajectories during treadmill walking from a representative non-neurologically impaired individual, presented as (a) a typical Butterfly diagram, and (b) density distribution.

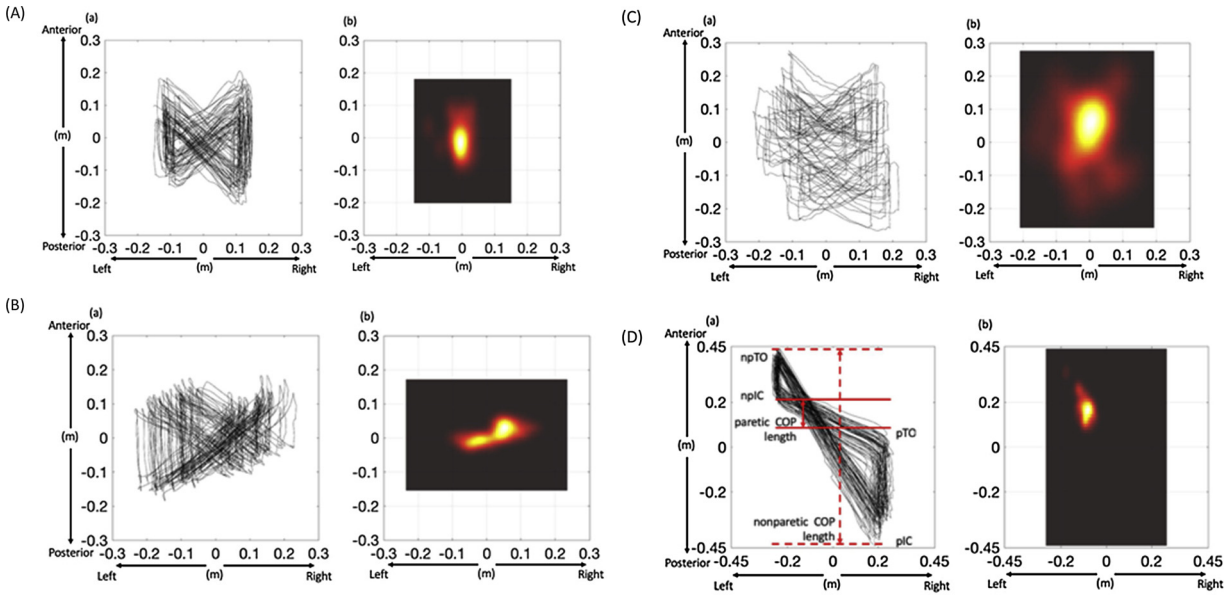

Fig. 2. The COP trajectories during treadmill walking from representative individuals with post-stroke hemiparesis, presented as typical Butterfly diagrams (a) and density distributions (b). (A) Pattern A; Participant_06. (B) Pattern B; Participant_01. (C) Pattern C; Participant_07. (D) Pattern D; Participant_08. pIC: paretic initial contact; pTO: paretic toe off; npIC: nonparetic initial contatc; npTO: nonparetic toe off.

$$COP_y = \frac{y_{left} F_{z-left} + y_{right} F_{z-right}}{F_{z-left} + F_{z-right}}$$

COP trajectory during walking was generated as a graphic pattern of "butterfly" (Fig. 1). Four key points of paretic and nonparetic IC and TO were determined(Fig. 2D), which were corresponding to the left and right sides in the control group, for the COP symmetry index calculation [13].

$$\text{COP symmetry index} = \frac{paretic\ COP\ length - nonparetic\ COP\ length}{paretic\ COP\ length + nonparetic\ COP\ length}$$

where paretic and non-paretic COP lengths were calculated as the absolute AP distance. The paretic COP length was between paretic TO (pTO) and consecutive nonparetic IC (npIC) while nonparetic COP length was between nonparetic TO (npTO) and consecutive paretic IC (pIC). In addition, the distances from pTO to npIC and npTO to pIC as well as the intersection between two lines of pTO-npIC and npTO-pIC were determined.

Standard deviations (SD) of step width, paretic step length, and non-paretic step length were used to represent variability of step width and lengths. The mean of step width, paretic step length, and non-paretic step length were also calculated.

For evaluation of variability, KDE was applied and calculated using the kde2d function from Botev et al. [23] in MATLAB. Coordinates, numbers of gait cycle, and maximum AP and ML range were used as inputs of the kde2d function. For each trial, the first and last three steps were removed to avoid the acceleration and deceleration effects in walking. In general, over 45 intersections were used for the calculation. The computation area was constructed within the maximum and minimum values of TO and IC for each participant. The maximum density was calculated and compared between groups.

Fig. 1 illustrates a typical butterfly diagram (Fig. 1a) and density distribution(Fig. 1b) from a non-impaired individual. The density distribution plot provides four pieces of information. First, the black box in Fig. 1b corresponds to the area of the COP trajectory, which is the area of the butterfly diagram in Fig. 1a. Second, the yellow region represents the highest density of intersection distribution and the location of COP trajectory area. Third, the red area immediately external to the yellow region represents how other intersections deviated from the point of highest density. Fourth, the vertical oval shape indicated that the distribution of intersections was mainly in the AP direction, versus the ML direction.

All parameters were averaged across all gait cycles for each participant for statistical comparisons. Using independent t-tests, we compared the COP symmetry index, the distances of pTO-npIC and npTO-pIC, highest density values, and mean and SD of step width, paretic step length and non-paretic step length between stroke-impaired and non-neurologically impaired groups. P values less than or equal to 0.05 were considered statistically significant.

3. Results

On average, self-selected walking speed for individuals post-stroke was 0.5 ± 0.26 m/s, which was significantly slower than that for non-impaired individuals (1.09 ± 0.25 m/s). Independent *t*-tests revealed that COP symmetry index and the distances of pTO-npIC and npTO-pIC were not significantly different between stroke-impaired and non-impaired groups. The COP symmetry index was -0.55 ± 0.94 in the stroke-impaired group versus -0.28 ± 0.10 in the non-impaired group ($t(18) = 0.917$, $p = 0.371$). Additionally, in the stroke-impaired group, distance of pTO-npIC was 0.38 ± 0.17 m, which was comparable to the distance from left TO to right IC (0.38 ± 0.04 m) in the non-impaired ($t(18) = -0.062$, $p = 0.951$). Similarly, the distance of npTO-pIC was 0.34 ± 0.09 m in the stroke-impaired and 0.35 ± 0.05 m (right TO to left IC) in the non-impaired ($t(18) = 0.149$, $p = 0.883$).

Independent t-tests revealed that mean step width, paretic step length, and non-paretic step length were different between groups, but not for SD of these variables (Table 1). The step width mean was significantly larger in the stroke-impaired compared to the non-impaired. Both means of paretic step length and non-paretic step length were significantly shorter compared to the left and right step length in the non-impaired. Additionally, the left and right step length in the non-impaired were evaluated by paired sample *t*-tests and showed no significant difference ($t(9) = 1.817$, $p = 0.103$). In the stroke-impaired, the paretic step length was significantly different and shorter compared to the non-paretic step length ($t(9) = 8.132$, $p < 0.001$).

The maximum value of the highest density was 275.33 ± 54.41 m^{-2} in the non-impaired, which was significantly larger than that in the stroke-impaired (96.11 ± 17.78 m^{-2}; $t(18) = 3.313$, $p = 0.006$). The AP and ML range as well as the location

Table 1
Means and standard deviations (SD) of step width, paretic step length, and non-paretic step length for both groups.

	Step width		Paretic step length (Left)		Non-paretic step length (Right)	
(cm)	Mean	SD	Mean	SD	Mean	SD
Stroke-Impaired	28.02 (8.68)	2.22 (1.25)	28.02 (8.68)	14.37 (7.30)	76.34 (21.14)	13.51 (6.79)
Non-Impaired	20.55 (3.08)	2.25 (0.75)	121.02 (23.30)	18.34 (8.19)	113.78 (12.34)	15.86 (6.31)
t	2.564	−0.051	−11.827	−1.145	−4.836	−0.801
p	**0.020**	0.960	< **0.001**	0.267	< **0.001**	0.434

Bolded p values denote statistically significant difference between groups ($p < 0.05$).

of intersection were used to categized patterns for neurological impaired individuals. Four different types of density distribution were categorized: Pattern A: similar AP and ML range (the intersection moved around the center) in Fig. 2A; Pattern B: larger ML than AP range (the intersection moved horizontally) in Fig. 2B; Pattern C: larger AP than ML range (the intersection moved vertically) in Fig. 2C; and Pattern D: larger AP than ML range (the intersection moved away from the center and skewed towards the paretic side) in Fig. 2D. The COP trajectory area and the location of the yellow region indicative of highest probability density of stroke-impaired Participant_06 (Fig. 2A, Pattern A) were comparable to that observed in the non-impaired group, but a broader yellow region indicative of highest probability density and red regions indicative of lower density was observed. In addition, the COP trajectory of stroke-impaired Participant_01 (Fig. 2B, Pattern B) was distributed more in the ML direction and stroke-impaired Participant_07 (Fig. 2C, Pattern C) in the AP direction. Additionally, the density of stroke-impaired Participant_07 (Pattern C) was lower and the intersections were distributed extensively around the COP trajectory area. Contrarily, the butterfly diagram of stroke-impaired Participant_08 (Fig. 2D) presented more consistent COP trajectory with higher maximum density compared to the other stroke-impaired participants. However, the COP trajectory area was also broader in both directions and the location of the yellow region indicative of highest probability density was away from the center and positioned towards the upper left corner (Fig. 2D, Pattern D).

Table 2 summarized the KDE patterns and highest density values for individuals with post-stroke hemiparesis. The average highest density value was 154.63 (45.53) m^{-2} for Pattern A, 108.85 (29.09) m^{-2} for Pattern B; 49.73 (14.02) m^{-2} for Pattern C, and 126.36 m^{-2} for Pattern D

4. Discussion

This study used a novel approach to evaluate locomotor variability in individuals with chronic post-stroke hemiparesis. Individuals with post-stroke hemiparesis presented comparable COP symmetry index and distances to non-impaired individuals. The density calculated using KDE was significantly smaller in the stroke-impaired versus the non-impaired group. KDE analysis not only provided the location and distribution field of intersections that differentiates between stroke- versus non-impaired walking, but also presented characteristically distinguishable patterns within the stroke-impaired group. In contrast, standard deviations of step width and step length did not differ between groups.

The butterfly diagram of the non-neurologically impaired individuals ranged from -0.1 ~ 0.1 m in the ML direction and from -0.2 ~ 0.2 m in the AP direction (Fig. 1), which were comparable with that reported previously [13]. In individuals post-stroke, symmetric butterfly diagrams have also been previously reported, consistent with our observations (Fig. 2A) [24]. The high variability in the stroke-impaired COP profiles may explain the lack of differences in the COP symmetry index and distances observed between stroke-impaired and non-impaired individuals.

Standard deviations of step width and step length have been used to represent locomotor variability [12,25,26]. This was supported in older adults with falls risks [26], but did not support that in individuals with post-stroke hemiparesis, where only a “trend towards significance” was reported by Balasurbramanian et al. [12]. In the current study, the SD values of step width and step length representing step width and length variability were not different between the non-impaired and stroke-impaired. Although step width variability was a more sensitive discriminating factor between older and young adults [25], it has also been reported that to accurately estimate step width variability (evaluation of standard deviation), at least 400 consecutive steps are required [27,28]. Together, this suggests that conventional measures of locomotor variability using standard deviation of step width and step length with smaller number of steps were not adequate in distinguishing locomotor variability between non-impaired and neurologically-impaired individuals.

To the best of our knowledge, this is the first study to apply KDE to evaluate locomotor variability on intersections of butterfly diagram in non-impaired gait, and furthermore, stroke-impaired gait. The primary outcome of KDE density was the distinctly smaller density in the stroke-impaired group compared to controls. Additionally, the smooth surface plots of KDE analysis highlighted the area of butterfly diagram, location of the highest density, distribution range, and distribution pattern. KDE revealed a highly consistent locomotor pattern in the non-impaired, in line with previous literature [14,16]. Individual KDE patterns and functional status for the stroke-impaired group are summarized in Table 2. Out of the 10 individuals with post-stroke hemiparesis, two presented Pattern A, with high variability of intersections; three participants presented Pattern B, likely due to poor lower extremity control

Table 2
KDE patterns and functional status for participants with post-stroke hemiparesis.

Participant ID	Age (y)	Time post stroke (y)	Paretic leg	Self-selected walking speed (m/s)	L/E FM score (/34)	Highest density ($1/m^2$)	KDE pattern type
01	69.02	7.99	Left	0.85	30	152.82	B
02	63.05	1.45	Left	0.60	30	200.16	A
03	63.04	7.96	Left	0.70	27	53.87	B
04	85.24	11.59	Left	0.23	25	119.85	B
05	77.15	0.67	Left	0.40	29	28.96	C
06	67.29	0.50	Left	0.70	30	109.11	A
07	77.02	29.12	Left	0.35	29	22.18	C
08	66.93	1.59	Left	1.10	30	126.36	D
09	83.14	5.43	Left	0.40	30	72.85	C
10	72.31	16.48	Left	0.55	24	74.92	C

resulting in foot landing positions biased towards ML direction; four participants presented Pattern C, likely due to poor lower extremity control resulting in foot landing positions biased towards AP direction, and one participant presented Pattern D, associated with low variability despite significant asymmetry between the paretic and non-paretic legs. Interestingly, although all individuals post-stroke exhibited hemiparesis, only Pattern D showed significant asymmetry between the paretic and non-paretic legs compared to the other patterns. Furthermore, these 4 characteristically different patterns within the stroke-impaired group are potentially associated with their functional capabilities or impairment levels, as suggested by their individual self-selected walking speeds and lower extremity Fugl-Meyer (L/E FM) scores summarized in Table 2. Specifically, individuals presenting with KDE Pattern A, which was similar to non-impaired but with lower density, and Pattern D, which had lower variability compared to other post-stroke patterns, both had higher self-selected walking speeds and L/E FM scores compared to individuals with KDE Pattern C. This supports our argument that distance comparisons would not adequately identify hemiparetic gait characteristics since there are considerable variabilities within the stroke-impaired population. A larger sample size will be needed for establishing the relationship between patterns and functional status of individuals post-stroke. Specifically, due to the large variability of stroke lesions, future studies will examine the different types of COP trajectories in participants across a wide spectrum of different functional levels.

5. Conclusions

Conventional presentations of locomotor COP trajectories using the butterfly diagram have limitations in describing variability post-stroke gait. This paper presents a novel approach of using KDE analysis as a better and more sensitive measure to characterize locomotor COP variability in individuals with post-stroke hemiparesis, compared to conventional measures.

Declaration of Competing Interest

The authors declare that they have no conflict of interest.

Acknowledgements

This work was supported in part by Ministry of Science and Technology in Taiwan (MOST107-2636-E-007-004) (YJL), and University of Nevada, Las Vegas, School of Integrated Health Sciences, Summer Research Fellowship (JNL).

The funding body does not play a role in the design of the study and collection, analysis, and interpretation of data or in writing the manuscript.

References

[1] J.M. Hausdorff, H.K. Edelberg, S.L. Mitchell, A.L. Goldberger, J.Y. Wei, Increased gait unsteadiness in community-dwelling elderly fallers, Arch. Phys. Med. Rehabil. 78 (3) (1997) 278–283 http://www.sciencedirect.com/science/article/pii/S0003999397900344.

[2] J.L. Allen, S.A. Kautz, R.R. Neptune, Step length asymmetry is representative of compensatory mechanisms used in post-stroke hemiparetic walking, Gait Posture 33 (4) (2011) 538–543.

[3] Y. Moon, J. Sung, R. An, M.E. Hernandez, J.J. Sosnoff, Gait variability in people with neurological disorders: a systematic review and meta-analysis, Hum. Mov. Sci. 47 (2016) 197–208.

[4] A. Kalron, Association between Gait Variability, Falls and Mobility in People With Multiple Sclerosis: a Specific Observation on the EDSS 4.0-4.5 Level, (2017).

[5] A.H. Snijders, N. van de Warrenburg, Bp Fau - Giladi, B.R. Giladi, N. Fau - Bloem, B.R. Bloem, Neurological Gait Disorders in Elderly People: Clinical Approach and Classification, (2019), pp. 1474–4422 (Print).

[6] R.L. Wright, J.W. Bevins, D. Pratt, C.M. Sackley, A.M. Wing, Metronome cueing of walking reduces gait variability after a cerebellar stroke, Front. Neurol. 7 (2016) 84.

[7] A. Guzik, M. Druzbicki, G. Przysada, M. Szczepanik, K. Bazarnik-Mucha, A. Kwolek, The use of the Gait Variability Index for the evaluation of individuals after a stroke, Acta Bioeng. Biomech. 20 (2) (2018) 171–177.

[8] A.E. Chisholm, S. Makepeace, E.L. Inness, S.D. Perry, W.E. McIlroy, A. Mansfield, Spatial-temporal Gait Variability Poststroke: Variations in Measurement and Implications for Measuring Change, (2019), pp. 1532–1821 X (Electronic)..

[9] J.N. Liang, D.A. Brown, Impaired foot-force direction regulation during postural loaded locomotion in individuals poststroke, J. Neurophysiol. 110 (2) (2013) 378–386 http://jn.physiology.org/content/110/2/378.long.

[10] J.M. Hausdorff, D.A. Rios, H.K. Edelberg, Gait variability and fall risk in community-living older adults: a 1-year prospective study, Arch. Phys. Med. Rehabil. 82 (8) (2001) 1050–1056 http://www.sciencedirect.com/science/article/pii/S0003999301632155.

[11] T.S. Wei, P.T. Liu, L.W. Chang, S.Y. Liu, Gait asymmetry, ankle spasticity, and depression as independent predictors of falls in ambulatory stroke patients, PLoS One 12 (5) (2017) e0177136.

[12] C.K. Balasubramanian, R.R. Neptune, S.A. Kautz, Variability in spatiotemporal step characteristics and its relationship to walking performance post-stroke, Gait Posture 29 (3) (2009) 408–414 http://www.sciencedirect.com/science/article/pii/S0966636208003585.

[13] F. Mawase, T. Haizler, S. Bar-Haim, A. Karniel, Kinetic adaptation during locomotion on a split-belt treadmill, J. Neurophysiol. 109 (8) (2013) 2216–2227.

[14] A. Kalron, L. Frid, The "butterfly diagram": a gait marker for neurological and cerebellar impairment in people with multiple sclerosis, J. Neurol. Sci. 358 (1-2) (2015) 92–100.

[15] C. Nuesch, J.A. Overberg, H. Schwameder, G. Pagenstert, A. Mundermann, Repeatability of spatiotemporal, plantar pressure and force parameters during treadmill walking and running, Gait Posture 62 (2018) 117–123.

[16] A. Kalron, Z. Dvir, L. Frid, A. Achiron, Quantifying gait impairment using an instrumented treadmill in people with multiple sclerosis, ISRN Neurol. 2013 (2013) 867575.

[17] K. Fukunaga, L. Hostetler, The estimation of the gradient of a density function, with applications in pattern recognition, IEEE Trans. Inf. Theory 21 (1) (1975) 32–40.

[18] A.Z. Zambom, R. Dias, A review of kernel density estimation with applications to econometrics, arXiv preprint arXiv 1212 (2812) (2012).

[19] Y. Chen, A tutorial on kernel density estimation and recent advances, Biostat. Epidemiol. 1 (1) (2017) 161–187.

[20] J.F. Bithell, An application of density estimation to geographical epidemiology, Stat. Med. 9 (6) (1990) 691–701.

[21] R.J. Marshall, A review of methods for the statistical analysis of spatial patterns of disease, J. R. Stat. Soc. 154 (3) (1991) 421–441.

[22] Z. Xie, Jun Yan, Kernel density estimation of traffic accidents in a network space, Computers, Enivorment and Urban Systems 32 (2008) 396–406.

[23] Z.I. Botev, J.F. Grotowski, D.P. Kroese, Kernel density estimation via diffusion, arXiv preprint arXiv 1011 (2602v1) (2010).

[24] A.M. Wong, Y.C. Pei, W.H. Hong, C.Y. Chung, Y.C. Lau, C.P. Chen, Foot contact pattern analysis in hemiplegic stroke patients: an implication for neurologic status determination, Arch. Phys. Med. Rehabil. 85 (10) (2004) 1625–1630.

[25] T.M. Owings, M.D. Grabiner, Step width variability, but not step length variability or step time variability, discriminates gait of healthy young and older adults during treadmill locomotion, J. Biomech. 37 (6) (2004) 935–938.

[26] M.L. Callisaya, L. Blizzard, M.D. Schmidt, K.L. Martin, J.L. McGinley, L.M. Sanders, et al., Gait, gait variability and the risk of multiple incident falls in older people: a population-based study, Age Ageing 40 (4) (2011) 481–487.

[27] T.M. Owings, M.D. Grabiner, Measuring step kinematic variability on an instrumented treadmill: how many steps are enough? J. Biomech. 36 (8) (2003) 1215–1218.

[28] D.M. Desmet, A. Sawers, M.D. Grabiner, Ensuring accurate estimates of step width variability during treadmill walking requires more than 400 consecutive steps, J. Biomech. 91 (2019) 160–163.